Fibers and Polymers 2010, Vol.11, No.8, 1146-1151 DOI 10.1007/s12221-010-1146-x

Crystal Structure and Thermal Properties of Poly(vinylidene fluoride)-Carbon Fiber Composite Films with Various Drawing Temperatures and Speeds

S. H. Lee and H. H. Cho[1]*

Department of Fashion Design, Dong-A University, Busan 604-714, Korea
[1]Department of Organic Material Science and Engineering, Pusan National University, Busan 609-735, Korea
(Received September 17, 2009; Revised June 3, 2010; Accepted August 16, 2010)

Abstract: PVDF-CF composite films were prepared using a melt pressing method. The PVDF-CF composite films were cut into rectangular shapes with a gauge length and width of 10 and 5 mm, respectively. The films were drawn using a universal testing machine equipped with a hot chamber. The drawing temperatures and speeds were 50~150 °C and 100~000 %/min, respectively. The crystal structure and physical properties of the resulting PVDF-CF films were investigated by wide angle X-ray diffraction, Fourier transform infrared spectroscopy, differential scanning calorimetry, dynamic mechanical analysis and scanning electron microscopy. The crystal form of the initial films was the <alpha> phase (non polarity, lamellar structure) of PVDF. The maximum draw ratio was 4.2. The drawn PVDF-CF films prepared at 100 °C were mainly the <beta> phase (polarity, fibrillar structure) of PVDF. With increasing drawing speeds, the <alpha> phase became the dominant phase of PVDF in the PVDF-CF films. The thermal properties of the PVDF-CF films improved with increasing drawing temperature, and the dynamic mechanical properties improved with increasing drawing speed.

Keywords: PVDF, Carbon fiber, Crystal structure, Thermal property

Introduction

Poly(vinylidene fluoride) (PVDF) [1] has attracted increasing interest for its piezoelectric, pyroelectric and ferroelectric properties. PVDF is a semicrystalline polymer with a high molecular weight and a ~50 % amorphous content. Five crystal structures are present in PVDF [2-5]. The electrical properties are associated with the <beta> phase, which has been found to induce polarity in the crystal structure. When PVDF is oriented uniaxially, it results in the longitudinal deformation of polymer chains in the crystals as well as increased <beta> phase formation [6].

Currently, PVDF composites have attracted the attention of many researchers [7-14]. PVDF with fillers such as fluorinated carbon black [7], piezoceramics [8], carbon nanofiber [9-11], TiO_2 [13], Graphene [14], Na^+-MMT [15], and MWCNT [16] have been widely studied. The concept of reinforcement is based on the fact that a low loading can result in a major change in the properties of PVDF. The mechanical properties, thermal properties and electrical conductivity can be improved with fillers, such as MWCNTs, SWCNT, and CNFs.

Carbon fiber reinforced polymer matrix composites [17] show high performance and advanced composite systems that are used in a multitude of applications encompassing, aerospace and aircraft structures, advanced marine vessels, oil field drilling risers, fuel cell components, natural gas fuel tanks, sports equipment, satellites, sensors, and others. In particular, the carbon fiber composite is a low cost material for energy applications [18]. Lee *et al.* [19] reported that pitch-carbon based carbon fibers exhibited a piezoresistive effect, in which the electric resistance of the carbon fiber changes under mechanical deformation, highlighting the possibility of carbon fiber-based pressure sensors.

In this study, the relationships between the fine structure and physical properties based on PVDF/carbon fiber (PVDF-CF) composite were investigated. The crystal structure and thermal properties of the PVDF-CF composite films under a range of processing conditions were examined. PVDF-CF films were prepared using a melt pressing method. The obtained PVDF-CF films were drawn uniaxially at various drawing speeds and temperatures. The properties were examined by wide angle X-ray diffraction (WAXD), Fourier transform infrared (FTIR) spectroscopy, differential scanning calorimetry (DSC), dynamic mechanical analysis (DMA) and scanning electron microscopy (SEM).

Experimental

Materials

The PVDF and PVDF-CF composite films were prepared using melt pressing methods. PVDF (SOLEF 1015, Solvay Co. Ltd.) and PVDF-CF composite chips (SOLEF 0902, Solvay Co. Ltd.) were pressed at 190 °C and 40 MPa for 5 min, followed by rapid quenching in ice water to obtain the PVDF and PVDF-CF composite films. The samples were prepared by compression molding using a 0.5 mm thick spacer.

Drawing Conditions

The PVDF and PVDF-CF composite films were cut into rectangular shapes with a gauge length and width of 10 and 5 mm, respectively. The films were drawn using a Shimazu AGS-500D Autograph equipped with a hot chamber at

*Corresponding author: hhcho@pusan.ac.kr

drawing temperatures of 50, 75, 100, 125, and 150 °C and speeds of 100, 200, 500, 2500, and 5000 %/min. After the pre-drawing test, the draw ratio of all samples was fixed to 4.

Characterizations

A high resolution SEM (JSM-35CF, Jeol, Japan) was used to observe the dispersion of CF in the PVDF matrix. The samples were dipped in liquid nitrogen for 3 min and the surface was fractured to avoid overcharging of the polymeric samples during SEM imaging.

WAXD (Rigaku Denki Co. Ltd.) was carried out using Ni-filtered Cu-Kα radiation (40 kV, 20 mA). The WAXD profiles were recorded along the equatorial and meridian directions using a fiber specimen attachment to a scintillation counter and pulse height analyzer.

FTIR (Nicolet 6700, thermoscientific USA) was recorded in the range from 500 to 4000 cm^{-1} using the attenuated total reflectance (ATR) method.

DSC was carried out over the temperature range, 30 to 230 °C, using a TA instrument at a heating rate of 10 °C/min. The sample weight was 3 mg.

DMA of the resulting films was analyzed in a sinusoidal oscillation using a non-resonant forced-vibration type viscoelastometer (Rheovibron, Model DDV-25FP, Orientec. Co.). The measurements were obtained between −70~150 °C at a heating rate of 5 °C/min.

Results and Discussion

Drawability and Surface Morphology of PVDF-CF Composite Films

Table 1 lists the maximum draw ratio of the pure PVDF and PVDF-CF films with various drawing temperatures and speeds. The resulting PVDF and PVDF-CF films were drawn up to the maximum draw ratio, which was fully propagated under various temperatures. In drawing at 50 °C, the draw ration of the pure PVDF films were ca. 4. With increasing drawing temperature to 150 °C, the draw ration increased to 4.5. The resulting PVDF-CF films were quite brittle at room temperatures. In drawing at 50 and 75 °C, the maximum draw ratio of the PVDF-CF films was <30 %. When drawing at 100 °C, the draw ratio was 3.9 and apparently homogeneous films were obtained. With increasing drawing temperature to 150 °C, the draw ratio increased to 4.2. With increasing drawing speed, the maximum draw ratio of PVDF-CF films was equal to 4.

Table 1. Drawability of the pure PVDF and PVDF-CF films with various drawing temperatures and speeds

Drawing temperatures at 100 %/min	DR_{max}		Drawing speeds at 125 °C	DR_{max}
	Pure PVDF	PVDF-CF		PVDF-CF
50 °C	4.1	-	100 %/min	4.1
75 °C	4.1	-	200 %/min	4.0
100 °C	4.0	3.9	500 %/min	4.0
125 °C	4.2	4.1	2500 %/min	4.0
150 °C	4.5	4.2	5000 %/min	4.0

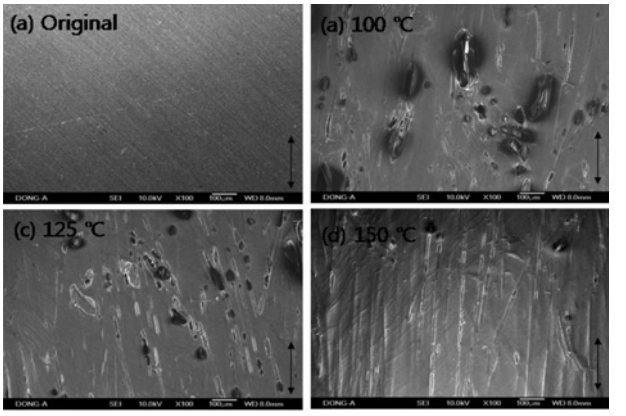

Figure 1. SEM images of the original and drawn PVDF-CF films with various drawing temperatures (↕; drawing direction).

Figure 1 shows SEM images of the surface of the original and drawn PVDF-CF films. The surface of the original PVDF films was clear. Carbon fibers were observed in the drawn PVDF-CF films. When the drawing temperature was increased to 150 °C, the orientation of the carbon fibers became parallel to the drawing direction.

Crystal Structure of PVDF-CF Composite Films

Figure 2 and 3 show the WAXD equatorial and meridional profiles of the pure PVDF and PVDF-CF composite films prepared with various drawing temperatures and speeds. The pure PVDF and original PVDF-CF films showed crystalline reflections at 17.8 °, 18.6 °, 26.7 °, and 37.8 ° 2θ in the equatorial and meridional scans. These peaks were assigned to the (100), (020), (101) and (002) planes of the <alpha>-form crystals of PVDF. The pure PVDF and original PVDF-CF films were crystalline and isotropic.

Generally, in an equatorial (EQ) scan, the reflections observed at 17.8 °, 18.4 °, 19.9 °, 26.5 °, and 38.0 ° 2θ were assigned to the (100), (020), (110), (021) and (002) reflections, respectively, of the <alpha> form crystal of PVDF. The peaks at 20 ° and 20.5 ° 2θ were assigned to the (110) and (200) reflections, respectively, of the <beta> form crystal. In the meridional (MD) scan, the PVDF peaks at 34.8 and 38.9 ° 2θ were assigned to the $(020)_\beta$ and $(002)_\alpha$ reflections, respectively. This suggests that the <beta> form PVDF crystal was the main crystalline structure of the drawn PVDF-CF films prepared at 100 °C. The crystallinity of the PVDF-CF films increased with increasing drawing temperature. At high drawing temperatures, crystals of the <alpha> and <beta> phases were observed in the MD scans. Drawing at high temperatures resulted in a decrease in the amount of the <alpha> to <beta> transition. Such a decrease may be related

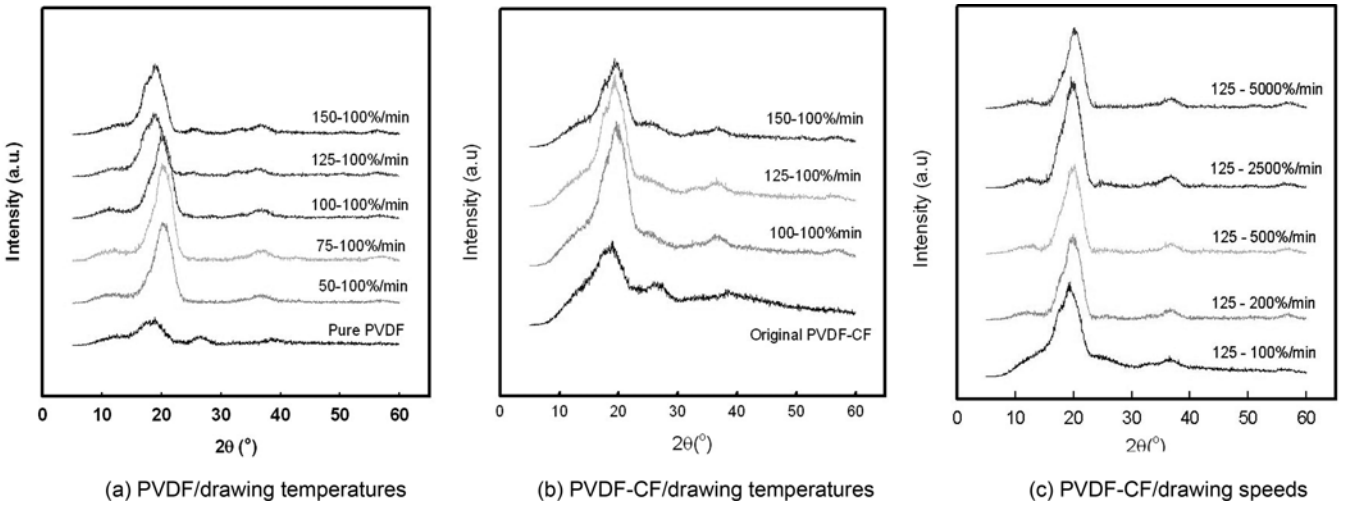

Figure 2. WAXD equtorial profiles of the pure PVDF and PVDF-CF films at various drawing temperatures (a, b) and speeds (c).

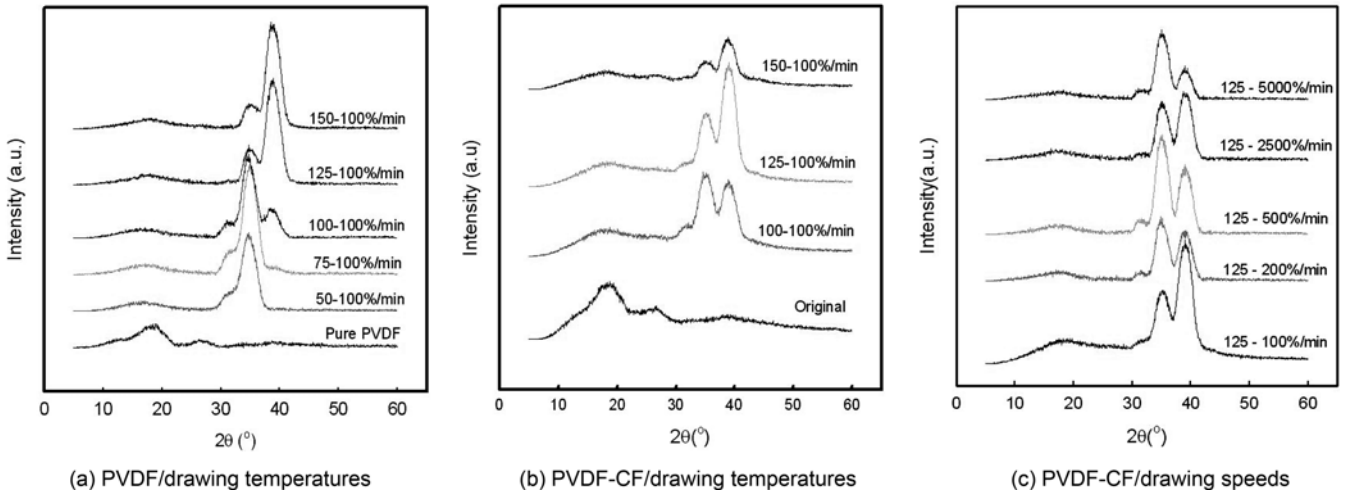

Figure 3. WAXD meridional profiles of the pure PVDF and PVDF-CF films at various drawing temperatures (a, b) and speeds (c).

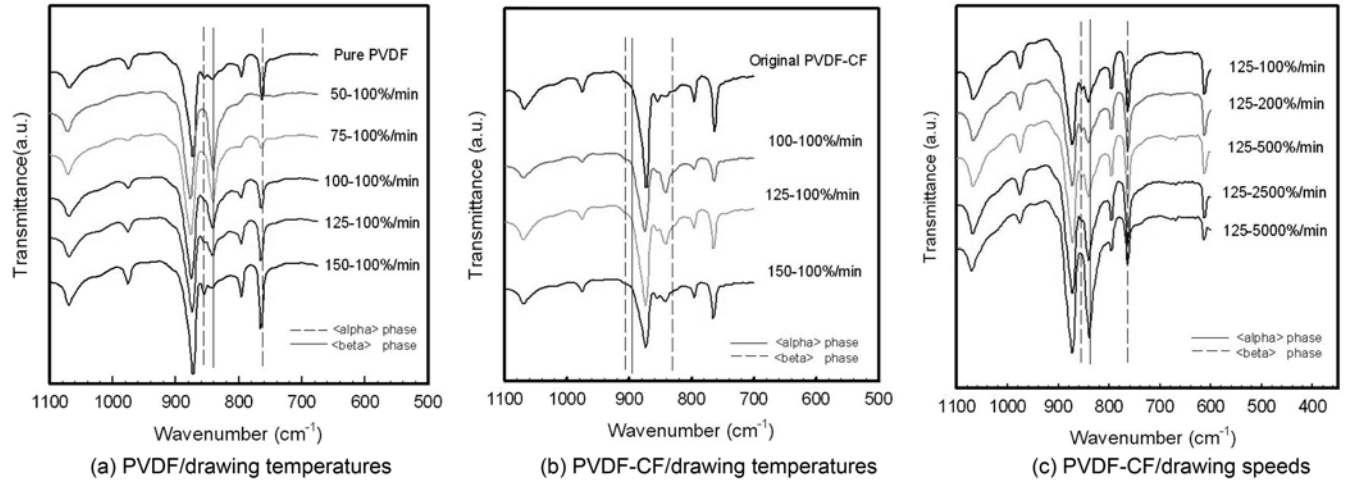

Figure 4. FTIR spectra of the pure PVDF and PVDF-CF films at various drawing temperatures (a, b) and speeds (c).

Table 2. Characteristic bands of PVDF with specific vibrational modes corresponding to the crystal structures [20]

	Wavenumber (cm^{-1})	Vibration mode
<alpha> phase of PVDF	531	CF_2 bending
	612	CF_2 bending and skeletal vibration of C-C-C
	766	In-plane bending or rocking
	855	Out of plane bending or rocking of CH_2
	976	-
<beta> phase of PVDF	510	CF_2 bending
	840	CH_2 rocking or CF_2 asymmetric stretching

to the decrease in drawing stress with increasing drawing temperature.

The crystal structure of pure PVDF and PVDF-CF films with increasing drawing temperature is very similar and seems to be no effect of carbon fiber in PVDF matrix.

For a drawing temperature of 125 °C, the PVDF-CF films with drawing speeds of 100~5000 %/min developed reflection peaks of the <alpha> and <beta> form (Figure 3(c)). In a drawing speed of 100 %/min, the $(002)_\alpha$ reflection peak became predominant. The $(020)_\beta$ reflection peak was observed at drawing speeds >200 %. In particular, at a drawing speed of 2500 %, the $(020)_\beta$ and $(002)_\alpha$ reflections peaks showed a similar intensity. Therefore, the two types of crystals coexist at various drawing temperatures.

Figure 4 shows the FT IR spectra of the the pure PVDF and PVDF-CF with various drawing temperatures. Gregori and Cestari [11] reported the IR absorption bands characteristic of the <alpha> phase (531, 612, 766, 795, 855, and 976 cm^{-1}), the <beta> phase (470, 511, and 840 cm^{-1}) for PVDF. Table 2 summarizes the characteristic bands of PVDF with specific vibrational modes corresponding to the crystal structures.

The IR band of the pure PVDF and original PVDF-CF films showed vibration modes characteristic of the <alpha> phase. At a drawing temperature of 100 °C, the absorbance at 840 cm^{-1} increased and was assigned to a mix mode of CH_2 rocking and CF_2 asymmetric stretching vibration that is parallel to the chain axis. This means that the crystal structure of drawn PVDF-CF films at 100 °C was the <beta> phase. With increasing drawing temperature to 150 °C, the IR band of the <alpha> phase was observed. At various drawing speeds at 125 °C, the characteristic IR band corresponding the <alpha> and <beta> phase was observed with increasing drawing speed. At a drawing speed of 2500 %/min, the 855 cm^{-1} band corresponding to the <alpha> phase weakened and the intensity of the 766 cm^{-1} related rocking vibration increased. In addition, the band at 840 cm^{-1} for the <beta> phase was strong.

WAXD and IR analysis suggests that the crystal structure of the drawn PVDF-CF films with increasing drawing temperature and speeds showed the co-existence of the <alpha>- and <beta> phases of PVDF in the PVDF-CF films. As the drawing temperature was increased, the <alpha> phase became dominant, whereas <beta> phase became dominant with increasing drawing speed. The <alpha> to <beta>-phase transformation of PVDF was reported to begin with necking. Necking marks the transformation from a spherulitic to micro fibrilar microstructure. Small blocks of lamella were torn away from the original lamellae to form a fibrillar structure of crystallites. This mechanism induces an all-trans planar zigzag conformation into the crystals characteristics of the <beta>-PVDF.

Thermal and Dynamic Mechanical Properties of PVDF-CF Composite Films

Figure 5 shows the DSC thermograms of the pure PVDF, original and drawn PVDF-CF with various drawing temperatures (a,b) and speeds (c) and Table 3 gives a

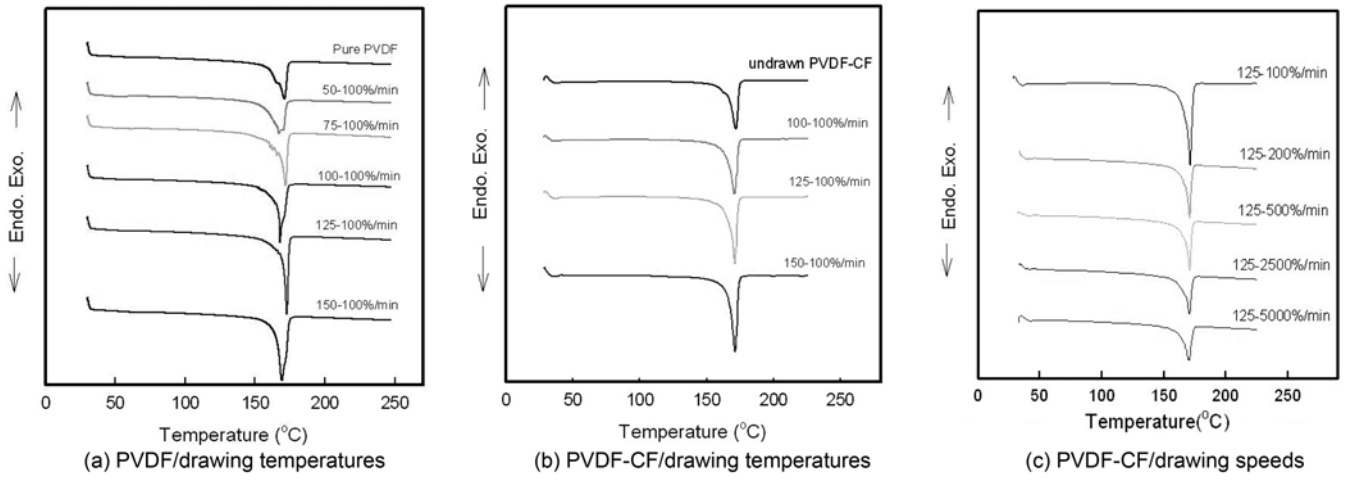

Figure 5. DSC thermograms of the pure PVDF and PVDF-CF films at various drawing temperatures (a, b) and speeds (c).

Table 3. Melting temperature and crystallinity of the pure PVDF and PVDF-CF films at various drawing temperatures and speeds

Drawing temperatures at 100 %/min	Pure PVDF			PVDF-CF			Drawing speeds at 125 °C	PVDF-CF		
	T_m (°C)	ΔH (J/g)	Xc (%)	T_m (°C)	ΔH (J/g)	Xc (%)		T_m (°C)	ΔH (J/g)	Xc (%)
Original	171.1	47.3	45.1	171.9	43.4	41.3				
50 °C	167.1	62.8	59.8	-	-	-	100 %/min	171.1	53.0	50.5
75 °C	171.9	60.4	57.5	-	-	-	200 %/min	170.7	55.2	52.6
100 °C	167.9	58.2	55.4	170.9	50.3	47.9	500 %/min	170.7	52.5	50.0
125 °C	172.8	56.6	53.9	171.1	53.0	50.5	2500 %/min	170.6	43.0	41.0
150 °C	169.3	68.2	65.0	171.4	60.0	57.1	5000 %/min	170.1	42.3	40.2

ΔH_{100} = 105 J/g.

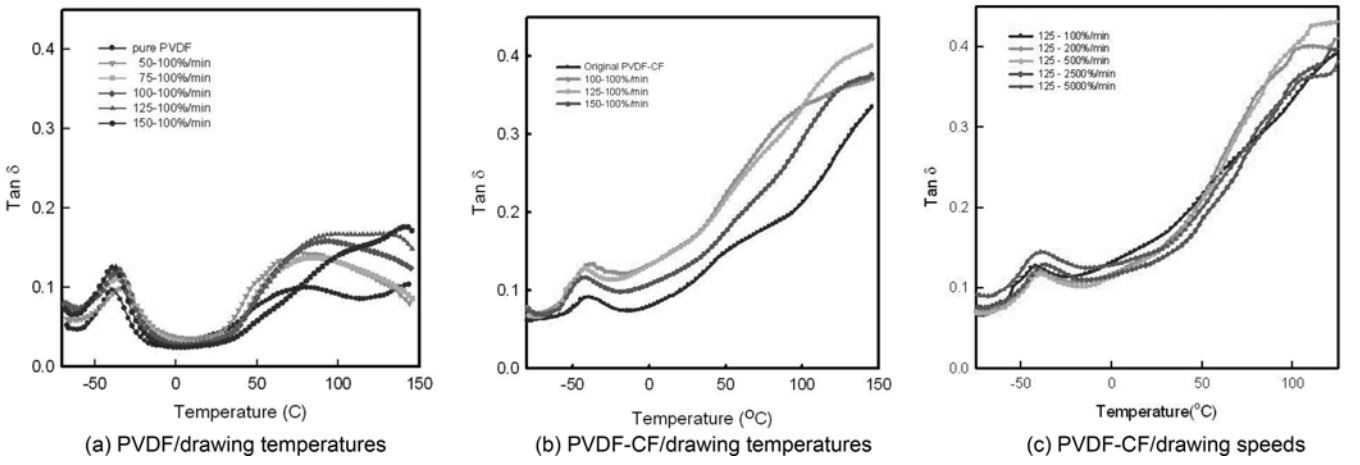

Figure 6. Tan δ of the pure PVDF and PVDF-CF films at various drawing temperatures (a, b) and speeds (c).

summary. The pure PVDF has a melting temperature of 171 °C and a melting enthalpy of 47.3 J/g. The original PVDF-CF films had a melting temperature of 171.9 °C and a melting enthalpy of 43.4 J/g. The melting point was unaffected by the drawing temperature. However, the melting enthalpy increased to 50.3 and 60.6 J/g. Therefore, the crystallinity of the PVDF-CF films increased with increasing drawing temperature. The PVDF-CF films resulted in significant increase in melting temperature comparing pure PVDF, but enthanlpy remained lower than the pure PVDF. That si, The carbon fiber enhance the nucleation efficiency of the PVDF matrix, the crytallinity decreased. In the case of various drawing speeds, the melting temperature of the drawn PVDF-CF films was similar but the crystallinity decreased. This shows that the crystal structure of the drawn PVDF-CF films contained a lower concentration of the <alpha> phase, which has a lamellar structure, and a higher concentration of the <beta> phase with a fibrilar structure and voids in the non crystalline regions.

Figure 6 shows the tan δ of the pure PVDF, original and drawn PVDF-CF with various drawing temperatures (a,b) and speeds (c). Table 4 lists the <beta>-transition and E' of the pure PVDF and PVDF-CF composite films prepared with various drawing temperatures and speeds. Theoretically, PVDF shows four main transitions observable in a typical DMA curve depending on the sample treatment [20,21]. The <gamma>-relaxation was attributed to chain rotation in the amorphous phase and is typically observed at approximately −80 °C. The <beta> relaxation was taken as the glass transition temperature normally observed at −40 °C. <beta> relaxation occurs in the amorphous phase of PVDF, which is attributed to fold motion and is usually observed at approximately 40 °C. <alpha> relaxation is believed to occur in the amorphous-crystalline interface region at approximately 80 °C.

In the Figure 6(a), the pure PVDF films exhibits two relaxations. The lower glass transition at approximately −42 °C is called <beta> relaxation corresponding to the amorphous phase and an upper glass transition corresponding to the amorphous crystalline at approximately 65 °C, which is known as <alpha> relaxation.

In the drawn PVDF-CF films, the lower T_g is shifted slightly toward a lower temperature indicating inhibited mobility. There was a significant decrease in peak height for the PVDF-CF films drawn at high drawing temperatures. The area under the amorphous transition is lower for PVDF-

Table 4. Dynamic mechanical behavior of original and drawn PVDF-CF films at various drawing temperatures and speeds

Drawing temperataures at 100 %/min	Pure PVDF			PVDF-CF			Drawing speeds at 125 °C	PVDF-CF		
	β-transition (°C)	E' (GPa)		β-transition (°C)	E' (GPa)			β-transition (°C)	E' (GPa)	
		at -25 °C	at 25 °C		at -25 °C	at 25 °C			at -25 °C	at 25°C
Original	-39.9	3.5	2.1	-39.3	6.4	4.3				
50 °C	-34.0	4.2	2.0				100 %/min	-42.4	2.7	1.7
75 °C	-34.4	3.6	1.9				200 %/min	-41.2	3.7	2.4
100 °C	-36.6	4.6	2.7	-38.2	4.1	2.5	500 %/min	-38.8	5.0	3.2
125 °C	-36.6	4.0	2.4	-42.4	2.7	1.7	2500 %/min	-36.9	5.3	3.3
150 °C	-36.9	3.6	2.3	-42.0	3.7	2.4	5000 %/min	-38.3	4.0	2.5

CF films, indicating either a higher level of crystallinity or a higher amount of interfacial polymer present.

The upper T_g relaxation was shifted towards a high temperature. With increasing drawing temperature, the drawn PVDF-CF films did not show a glass transition temperature within the range investigated. With increasing drawing speeds, the peaks of the <beta>-transition was shifted a higher temperature. The PVDF-CF films prepared at 125 °C and a speed of 2500 %/min showed an E' value of 3.3 Gpa at 25 °C.

Conclusion

Poly(vinylidenefluoride)-carbon fiber composite films were prepared using a melt pressing method. The resulting PVDF-CF films were drawn uniaxially at 100, 125, and 150 °C, and different drawing speeds. The maximum draw ratio was 4.2 at a drawing temperature of 150 °C. The crystal form of the initial PVDF-CF films was the <alpha> phase (non polarity) of PVDF. The drawn PVDF-CF films prepared at 100 °C were mainly the <beta> phase(polarity) of PVDF. With increasing drawing speed, the <alpha> phase became the dominant phase of PVDF in PVDF-CF films. The thermal properties of the PVDF-CF films improved with increasing drawing temperature. The PVDF-CF films prepared at 125 °C and speed of 2500 %/min had an E' value 3.3 Gpa at 25 °C.

Acknowledgement

This study was supported by research funds from Dong-A University in 2010. Authors were indebted to Prof. Takeshi Kikutani (Tokyo Institute of Technology, Japan) for helpful advices.

References

1. J. E. Mark, "Physical Properties of Polymers Handbook", p.509, American Institute of Physics, Woodbury, New York, 1996.
2. R. Hasegawa, Y. Takahashi, Y. Chatani, and H. Tadokoro, *Polym. J.*, **3**, 600 (1972).
3. S. Weinhold, M. H. Fitt, and J. B. Lando, *Macromolecules*, **13**, 1178 (1980).
4. A. J. Lovinger, *Macromolecules*, **14**, 322 (1981).
5. Y. Takahashi, Y. Matsubara, and H. Tadokoro, *Macromolecules*, **16**, 1588 (1983).
6. B. Mohannadi, A. A. Yousefi, and S. M. Bellah, *Polym. Test*, **26**, 42 (2007).
7. G. Wu, C. Zhang, T. Miura, S. Asai, and M. Sumita, *J. Appl. Polym. Sci.*, **80**, 1063 (2001).
8. A. Seema, K. R. Dayas, and J. M. Varghese, *J. Appl. Polym. Sci.*, **106**, 146 (2007).
9. S. Vidhate, A. Shaito, J. Chung, and N. A. D'souza, *J. Appl. Polym. Sci.*, **112**, 254 (2009).
10. T. Danno, H. Matsumoto, M. Nasir, M. Minagawa, H. Horibe, and A. Tanioka, *J. Appl. Polym. Sci.*, **112**, 1868 (2009).
11. P. Costa, J. Silvia, V. Sencadas, C. M. Costa, F. W. J. Van Hattum, J. G. Rocha, and S. Lanceros-Mendez, *Carbon*, **47**, 2590 (2009).
12. L. Y. Yu, H. M. Shen, and Z. L. Xu, *J. Appl. Polym. Sci.*, **113**, 1763 (2009).
13. S. Ansari and E. P. Giannelis, *J. Polym. Sci., Polym. Phys.*, **47**, 903 (2009).
14. T. Wu, T. Xie, and C. Yang, *J. Polym. Sci., Polym. Phys.*, **47**, 888 (2009).
15. L. He, Q. Xu, C. Hua, and R. Song, *Polym. Composite*, DOI 10.1002/pc.20876 (2009).
16. Y. W. Nam, W. N. Kim, Y. H. Cho, D. W. Chae, G. H. Kim, S. P. Hong, S. S. Hwang, and S. M. Hong, *Macromol. Symp.*, **249**, 478 (2007).
17. J. H. Koo, "Polymer Nanocomposites -Processing, Characterization, and Applications-", p.198, McGraw-Hill, New York, 2006.
18. P. Morgan, "Carbon Fiber and Their Composite", p.75, CRC Press, Cambridgeshire, UK, 2005.
19. C. S. Park, B. S. Kang, and D. W. Lee, *Transactions of the KSME A*, **31**, 417 (2007).
20. N. Mekhilef, *J. Appl. Polym. Sci.*, **80**, 230 (2001).
21. A. J. Lovinger, "In Development in Crystalline Polymers", Applied Science Publishers, London, 1982.